

Clustering of Photometric Luminous Red Galaxies II: Cosmological Implications from the Baryon Acoustic Scale

A. Carnero¹, E. Sánchez^{1*}, M. Crocce², A. Cabré³, E. Gaztañaga²

¹*Centro de Investigaciones Energéticas, Medioambientales y Tecnológicas (CIEMAT), Madrid, Spain*

²*Institut de Ciències de l'Espai (IEEC-CSIC), Barcelona, Spain*

³*University of Pennsylvania, Philadelphia, USA*

22 August 2022

ABSTRACT

A new determination of the sound horizon scale is presented. It makes use of $\sim 1.5 \times 10^6$ luminous red galaxies, selected from the Sloan Digital Sky Survey imaging data, with photometric redshifts. The sample is selected at redshifts that go from 0.4 to 0.6. We find evidence of the Baryon Acoustic Oscillations (BAO) signal at the $\sim 2.3\sigma$ level, at the highest redshift to date, $0.50 < z < 0.60$. We obtain a value of $\theta_{BAO}(z = 0.55) = (3.90 \pm 0.38)^\circ$ for the angular BAO scale, including systematic errors. This is the first direct measurement of the angular BAO signal. We show its complementarity with the radial determination and how the degeneracy in the determination of cosmological parameters is broken when both measurements (angular and radial) are combined. The measurement is in good agreement with the expectations from the WMAP7 best-fit cosmology. Combining with previous measurements of the acoustic scale, we obtain a value of $w_0 = -1.03 \pm 0.16$ for the equation of state parameter of the dark energy, or $\Omega_M = 0.26 \pm 0.04$ for the matter density, when the other parameters are fixed. Both values include systematic errors. We have also tested the sensitivity of current BAO measurements to a time varying dark energy equation of state, finding $w_a = 0.06 \pm 0.22$, including systematics and with the other parameters fixed.

Key words: data analysis – cosmological parameters – dark energy – large-scale structure of the universe

1 INTRODUCTION

The signal that the baryon acoustic oscillations (BAO) leave in the distribution of galaxies was discovered in 2005 (Eisenstein et al. 2005), using the Sloan Digital Sky Survey (SDSS)¹ data (York et al. 2000). Since then, several more detections at different redshifts have been performed (Percival et al. 2007; Sánchez et al. 2009; Gaztañaga et al. 2009; Reid et al. 2010; Percival et al. 2010; Kazin et al. 2010). All these detections used spectroscopic determinations of the redshifts of the galaxies, which has been the traditional technique to estimate distances, and measure the cosmological parameters through an averaged three-dimensional evaluation of the galaxy clustering, including the influence of BAO. The purely radial BAO signal was measured for the first time in Gaztañaga et al. (2009), and determines the redshift intervals that correspond to the sound horizon scale at two different redshifts. There are ongoing or proposed projects

like BOSS (Schlegel et al. 2007) or BigBOSS (Schlegel et al. 2009) that will use massive measurements of galaxy spectra to obtain new measurements of the BAO scale, more precise and deeper than current determinations.

The feasibility of measuring the BAO signal using photometric redshifts was first demonstrated in Padmanabhan et al. (2007) (see also Blake et al. (2007) and Thomas et al. (2011)). Large multiband imaging surveys are a powerful way to explore the clustering properties of galaxies. Their advantage is the possibility of mapping wider areas in deeper volumes compared with spectroscopy. However, the precision of the photoz is worse than its spectroscopic counterpart. There are projects like DES (The Dark Energy Survey Collaboration 2005), PanSTARRS (Kaiser et al. 2000) or LSST (Tyson et al. 2003) that aim to obtain the most precise cosmological constraints using purely photometric surveys, compensating the lack of precision in the redshift determination with the larger volume of the survey, the larger density of galaxies and the possibility of analysing different galaxy populations.

In this paper, a new determination of the BAO scale

* E-mail: eusebio.sanchez@ciemat.es

¹ <http://www.sdss.org>

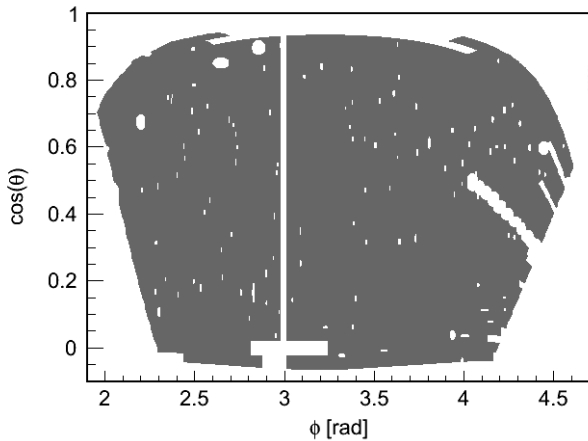


Figure 1. The mask used in this analysis. The white regions are excluded of the analysis. The spherical coordinates are related to the equatorial coordinates as $\phi = ra$ and $\theta = (\pi/2 - dec)$. The vertical band at $\phi \sim 3$ is due to the photo- z used in this analysis.

is presented. The measurement uses the photometric sample of Luminous Red Galaxies (LRG) in the SDSS seventh data release (DR7) published by Abazajian et al. (2009). We make use of the features of photometric redshift surveys and explore the BAO signal at the highest redshift to date, $z = 0.55$. Moreover, this is the first direct measurement of the purely angular BAO signal. It is complementary to the purely radial and to the three-dimensional averaged signal of BAO, and contributes to break degeneracies in the determination of cosmological parameters.

We use a model independent determination (Sánchez et al. 2011) of the angular BAO scale, by means of a simple method to localize it with precision. The method is based on a parametrization of the angular correlation function as a sum of a power law, a constant and a Gaussian. There are a total of 6 parameters and the BAO position and its significance are given by the location and S/N in amplitude of the Gaussian. It is robust against systematic errors, uses only observable quantities and is independent of any assumption about other parameters or the shape of the correlation function. We also evaluate the systematic errors associated to the measurement.

The paper is organized as follows. First, we briefly present the selection of the LRG sample, that is common with the companion paper Crocce et al. (2011). Then, the measured angular correlation functions are discussed. Finally, we present the results about the BAO scale and obtain some cosmological constraints from them, finishing with the conclusions.

2 SELECTION OF THE GALAXY SAMPLE

We perform a color based selection of LRG in the SDSS-DR7 imaging sample, based on that published by Cabré et al. (2006). The selection is described in more detail in the companion paper Crocce et al. (2011). First, we select the region in the color-color space that is populated by LRG (Eisenstein et al. 2001), requiring $(r-i) > \frac{(g-r)}{4} + 0.36$ and $(g-r) >$

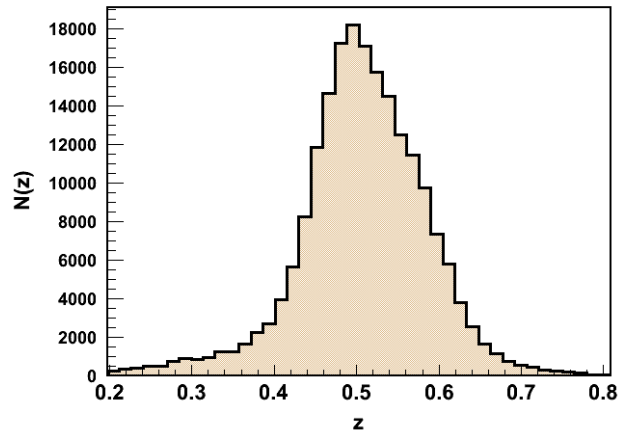


Figure 2. True distribution with redshift of the galaxies selected as LRG. The distribution has been obtained summing the full PDFs of the selected galaxies.

$-0.72 (r - i) + 1.7$. Then, we minimise the star contamination, imposing an additional set of cuts: $17 < r_{Petro} < 21$, $0 < \sigma_{r_{Petro}} < 0.5$, $0 < (r - i) < 2$, $0 < (g - r) < 3$ and $22 \text{ mag arcsec}^{-2} < \mu_{50} < 24.5 \text{ mag arcsec}^{-2}$. In these cuts, g , r and i are the model magnitudes corrected by extinction, $\sigma_{r_{Petro}}$ is the error on the Petrosian magnitude r_{Petro} and μ_{50} is the mean surface brightness within the Petrosian half-light radius in the r band. Finally, only galactic latitudes $b > 25^\circ$ are considered. A total of $\sim 1.5 \times 10^6$ objects are selected, with a star contamination of $4 \pm 1\%$, determined using the spectroscopic SDSS sample.

We use the angular mask depicted in Figure 1, where $\phi = ra$ and $\theta = \pi/2 - dec$, and ra , dec are the equatorial coordinates. We have included only the largest contiguous area of the survey. There is a vertical band at $\phi \sim 3$ that is excluded due to the photo- z catalogue we have used, described in the next section. A total area of 7136 square degrees is considered. We have verified that the angular mask is valid in the full redshift range used in this analysis. For further details, see Crocce et al. (2011).

3 CORRELATION FUNCTIONS

The photometric redshift determination developed in Oyaizu et al. (2008) is used in this analysis. It is combined with the value added catalogue of Cunha et al. (2009), where the photometric redshift probability distribution function (PDF) for every object is given, following the method of Lima et al. (2008). We determine the redshift for each object as the maximum of its PDF, but the full PDF distribution is used to estimate the true distribution of objects with redshift, which is shown in Figure 2. Objects with a PDF distributions that do not satisfy good quality requirements are rejected (see Crocce et al. (2011) for a detailed description of the photometric redshift quality requirements). The most populated region of redshift, from 0.4 to 0.6 is considered in this measurement. Outside this region the statistics is very small to make an observation of the BAO scale.

We divide the range in two redshift bins, centred at $z = 0.45$ and $z = 0.55$, and both with a width of $\Delta z_{phot} = 0.1$.

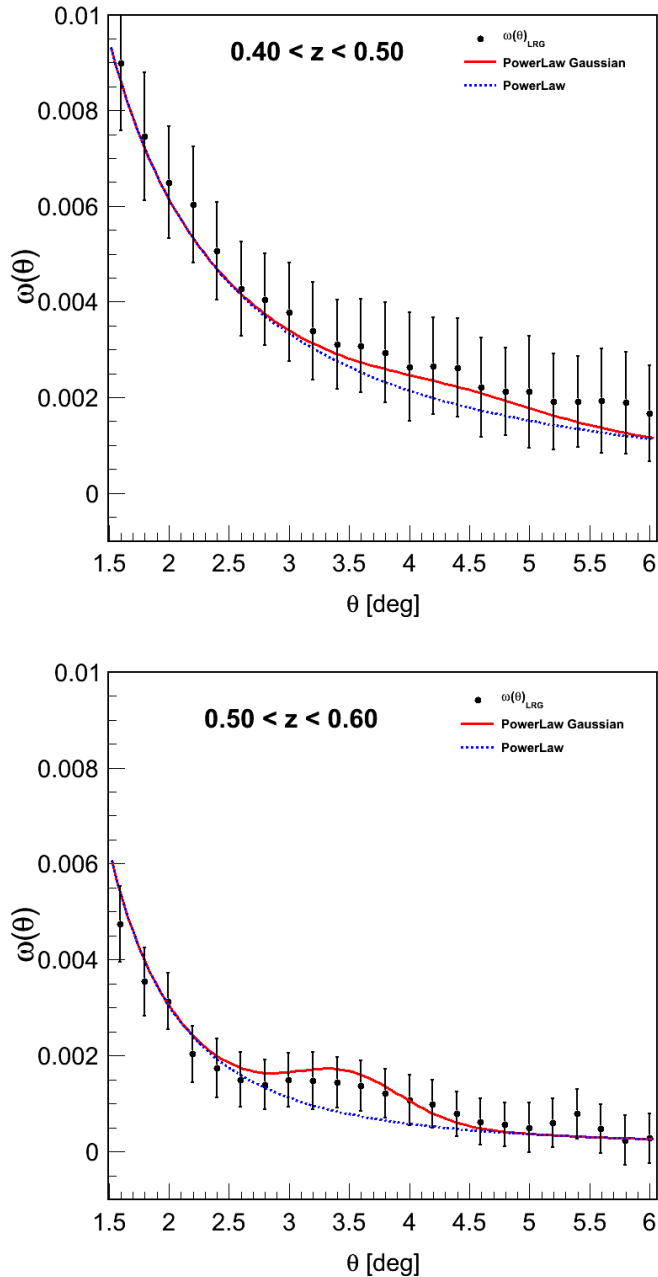


Figure 3. The observed correlation functions for the two analysed redshift bins: $\omega(\theta, z = 0.45)$ (top), and $\omega(\theta, z = 0.55)$ (bottom). The solid lines are the result of fitting the functions to a power law plus a Gaussian, following the method presented in Sánchez et al. (2011), including the covariance matrix. The dotted lines show only the power law. The correlation function at $z = 0.45$ is well described by only the power law, while the correlation function at $z = 0.55$ needs the peak with a statistical significance of 2.3σ .

The number of objects in each bin is 0.47×10^6 and 0.61×10^6 , respectively. We have found these bins to be the optimal choice. Much narrower bins do not enhance the sensitivity, due to the dilution effect of the photometric redshift. On the other hand, much wider bins make the amplitude of the correlation function too small to detect the BAO signal due

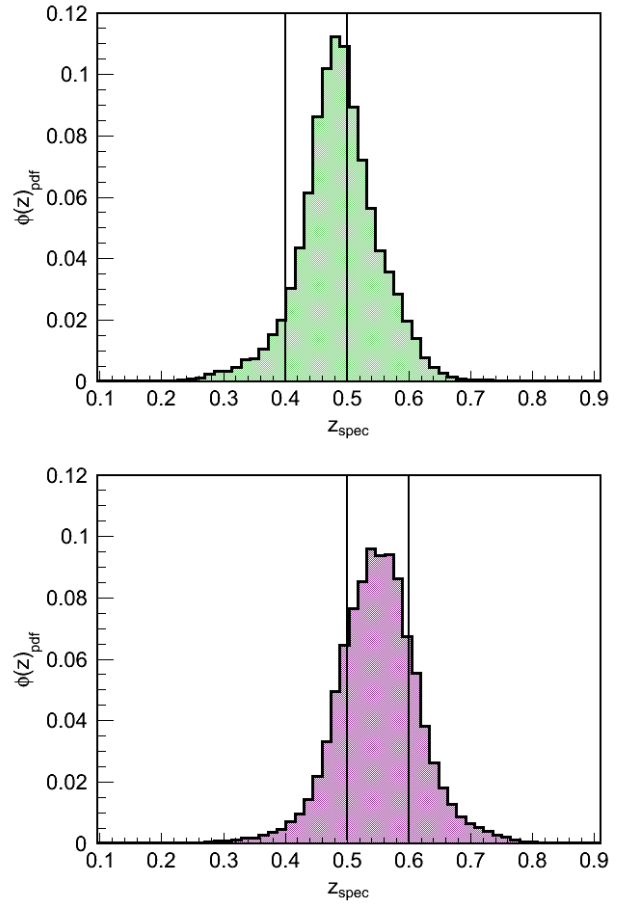


Figure 4. True distribution of galaxies with redshift for the two used bins: $z = 0.45$ (top), and $z = 0.55$ (bottom). These distributions have been obtained summing the full PDFs for all the galaxies selected in each bin. The distribution for $z = 0.45$ is asymmetric and has some bias, since its center is not at 0.45. The distribution for $z = 0.55$ is well-behaved. The vertical lines correspond to the limits of the bin for the photometric redshift.

to the projection effect. The Figure 3 shows the measured angular correlation functions for these two bins (dots). They have been computed using the Landy & Szalay (Landy & Szalay 1993) estimator.

The error and covariances in the observed correlation functions have been evaluated using three independent methods. First, we have generated 50 artificial realizations of these correlation functions, and compute the error as the dispersion of the realizations. Second, we have used the Jack-Knife method, dividing the area in 80 regions. And third, we have used the theoretical description, following the result in Croce et al. (2010). The three determinations are in perfect agreement. To see a more detailed discussion of the error calculation, see Croce et al. (2011).

4 RESULTS

We use the method described in Sánchez et al. (2011) to measure the BAO scale using the observed correlation functions presented in the previous section. Results of fitting $\omega(\theta)$ to a power law plus a Gaussian, including the full

Systematic error	$\Delta\theta_{BAO}$
Parametrization	1%
Photometric redshift error	5%
Redshift space distortions	1%
Theory	1%
Projection effect	1%
Photometric redshift algorithm	2%
Selection of the Sample	2.5%
Survey mask	2%

Table 1. Estimation of systematic errors in the determination of θ_{BAO} . Those above the horizontal line are taken from Sánchez et al. (2011). The others are the main new contributions that arise from a real photometric redshift survey.

covariance matrices (introduced in the companion paper Croce et al. (2011)), are presented in Figure 3 (solid lines), and compared to only the power law (dotted lines).

The BAO peak is detected at $z = 0.55$, with a statistical significance of 2.3 standard deviations. However, we have no evidence of peak for $z = 0.45$. This is not surprising, since the quality of the photometric redshift is poorer in this region, as shown in Figure 4. The distribution of galaxies in the $z = 0.45$ bin, obtained using the full PDF, is not centred at $z = 0.45$. Moreover, it is asymmetric, making the true width of the bin wider. These effects add, making impossible a statistically significant detection of the BAO peak. The $z = 0.55$ bin, however, shows a well-behaved distribution.

4.1 Systematic Errors

The main systematic errors affecting this measurement have been described in Sánchez et al. (2011) and are used here. There are, however, some additional effects that need to be taken into account. First, those effects related to the selection of the sample (selection cuts, mask and contamination). Second, a possible larger influence of the photometric redshift, since it is not perfectly ideal as supposed in Sánchez et al. (2011).

To evaluate the systematic error associate to the selection of the sample we have varied the selection cuts within 10% of their nominal values of the section 2. The maximum variation found is $\Delta\theta_{BAO}(selection) = 2.5\%$, and is assigned as the systematic error due to the sample selection. We have also varied the mask, relaxing the excluded regions. Results are stable within 2%, that is assigned as the systematic error associated to the mask: $\Delta\theta_{BAO}(mask) = 2\%$.

The influence of the star contamination has also been checked. It is found to be negligible, since the correlation function of the stars varies very slowly with the angle, and the fit is able to describe this contribution.

The effect of the photometric redshift has been evaluated computing the BAO scale with different estimations of redshifts, contained in the SDSS DR7 catalogue. We have found results that are consistent within 2%. Therefore, we add a contribution to the systematic error of $\Delta\theta_{BAO}(photoz) = 2\%$, fully correlated with the systematic error due to the photometric redshift error, described in Sánchez et al. (2011).

The full accounting of systematic errors is presented in Table 1. The total systematic error is $\Delta\theta_{BAO}(sys) = 8.0\%$.

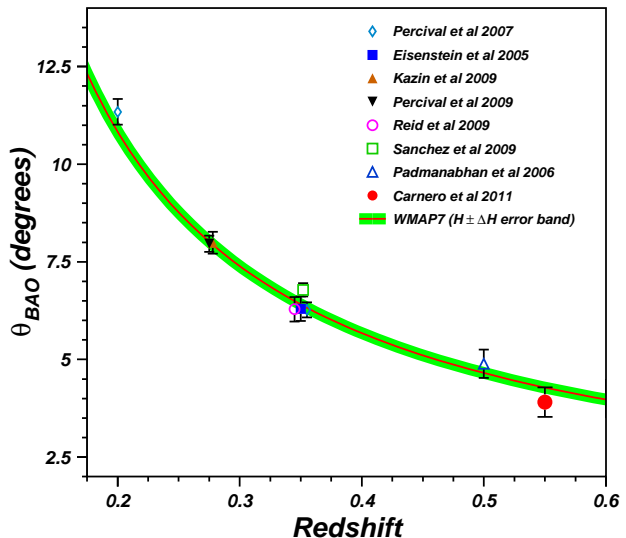


Figure 5. Evolution with the redshift of the angular BAO scale. The measurement presented in this paper is the solid dot. Its error includes both the statistical and the systematic contributions. The other measurements are inferred from the given reference by translating the three-dimensional averaged distance parameter D_V into an angular scale, with the fiducial cosmology used in each reference. All of them are compatible with the WMAP7 cosmology (solid line). The band includes the uncertainty in the Hubble constant H_0 . Some of the measurements at $z = 0.35$ have been slightly displaced in redshift for clarity.

4.2 Comparison with Previous Measurements

The fitted value for the angular scale associated to the BAO is $\theta_{FIT} = 3.48 \pm 0.19^\circ$, at $z = 0.55$ and $\Delta z_{photo} = 0.1$. Following Sánchez et al. (2011), this value must be corrected to obtain the BAO angular scale, $\theta_{BAO} = \alpha(z, \Delta z)\theta_{FIT}$. For this redshift and bin width, the correction is $\alpha(z = 0.55, \Delta z_{true} = \sqrt{2\pi}\Delta z_{photo}) = 1.12$. The final result for the BAO scale, including statistical and systematic errors, is $\theta_{BAO}(z = 0.55) = 3.90 \pm 0.38^\circ$.

The variation of the measured angular BAO scale with the redshift is presented in Figure 5. The measurement presented in this analysis is the solid dot, and includes the statistical and the systematic errors contribution. The other measurements are inferred from the given reference by translating the three-dimensional averaged distance parameter D_V into an angular scale, with the fiducial cosmology used in each reference. All the measurements are in agreement with the WMAP7 cosmology, represented by the solid line. The band includes the uncertainty in the determination of the Hubble constant H_0 (Riess et al. 2011).

We have performed a test to obtain the sensitivity of all the BAO determinations up to date to a dark energy with an equation of state parameter that varies with time, as $w(a) = w_0 + w_a(1 - a)$, where a is the scale factor of the universe. The Figure 6 (Left) shows the allowed regions for the parameters w_0 and w_a , when we fit the evolution of the BAO scale with redshift using the Figure 5 and the radial BAO scale determinations at redshifts $z = 0.24$ and $z = 0.43$

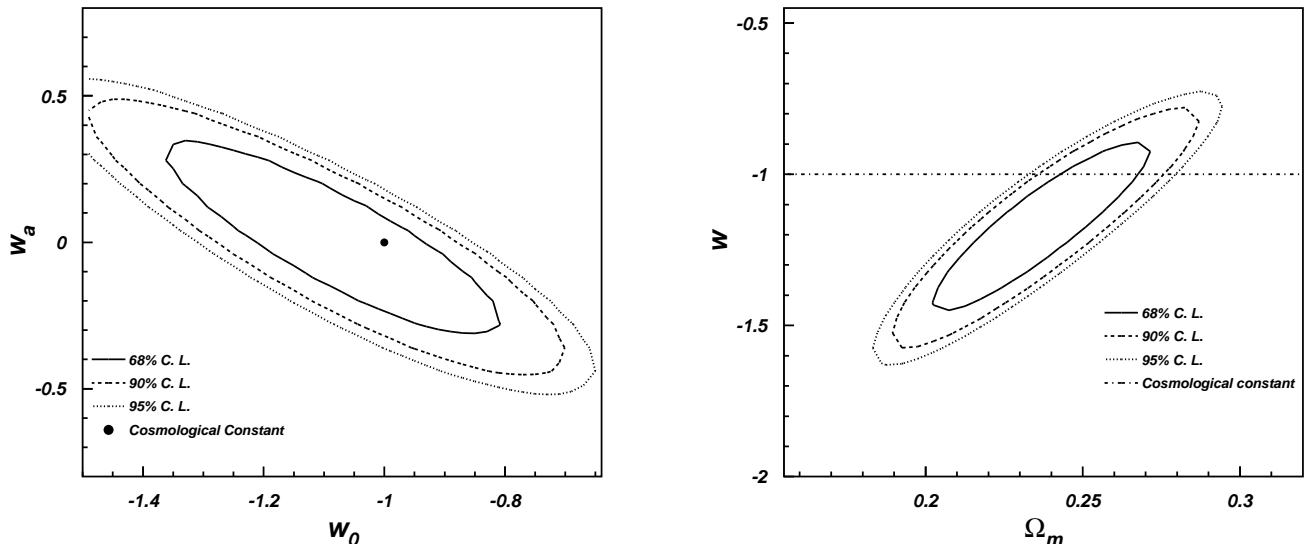


Figure 6. Constraints in the properties of the dark energy from data in the Figure 5 and the radial BAO from Gaztañaga et al. (2009). Left: Constraints in the plane w_0 , w_a , where $w(a) = w_0 + w_a(1 - a)$, and a the scale factor of the universe. Data are compatible with dark energy being a cosmological constant (solid dot). Right: Constraints in the plane w , Ω_m . Results are compatible with previous determinations. The dash-dotted line corresponds to the dark energy being a cosmological constant and is compatible with the measurement.

from Cabré & Gaztañaga (2011). We fix all the other parameters to their values for the WMAP7 w CDM cosmology (Komatsu et al. 2011), and use the most recent Hubble constant determination (Riess et al. 2011). We have chosen the points of Percival et al. (2007) at $z = 0.20$, Percival et al. (2010) at $z = 0.275$, Sánchez et al. (2009) at $z = 0.35$ and the measurement presented in this paper at $z = 0.55$, since measurements at the same or similar redshifts are strongly correlated. Data are compatible with dark energy being a cosmological constant ($w_0 = -1$, $w_a = 0$, included as the solid dot).

We have also checked the sensitivity of these data in the plane w , Ω_m . The result is presented in the Figure 6 (Right). The dash-dotted line shows the expected value for the dark energy being a cosmological constant, and is perfectly compatible with data. The determination is compatible with previous determinations using the radial BAO measurements (Gaztañaga et al. 2009).

The fit to a single parameter gives $w = -1.03 \pm 0.16$. The data are compatible with a cosmological constant with a precision of $\sim 20\%$. If we do the same study for Ω_m , we find a value of $\Omega_M = 0.26 \pm 0.04$. Both measurements include the systematic errors, and have been obtained fixing all the other parameters to the same values than above, except H_0 , which has been varied within its uncertainty.

The influence of the new determination at $z = 0.55$ is shown in Figure 7 (Left), where we compare the constraints at 68% C. L. for all the data (bold) with the constraints obtained when the point at $z = 0.55$ is excluded (light). The contribution of the new point is not negligible, since its inclusion makes the constraints more precise. Moreover, we have studied how angular determinations of BAO and radial determination of BAO contribute to the cosmological constraints. This is depicted in Figure 7 (Right), where the

light vertical contour corresponds to the angular BAO scale determinations and the light diagonal contour corresponds to the radial BAO measurements. The bold contour are the full combination at 68% C. L., also presented in Figure 6 (Right). Both determinations are complementary and the combination clearly breaks degeneracies between cosmological parameters, enhancing the sensitivity.

5 CONCLUSIONS

We have measured the BAO signal in the distribution of galaxies at the highest redshift to date, $0.5 < z < 0.6$, using a LRG sample selected from the SDSS DR7 photometric catalogue. The BAO signal is detected with a statistical significance of 2.3 standard deviations, as expected from the characteristics of the sample (Cabré & Gaztañaga 2011). The result is in agreement with the WMAP7 cosmology. We find $\theta_{BAO}(z = 0.55) = (3.90 \pm 0.38)^\circ$ for the angular BAO scale, including systematic errors. Combining with previous BAO measurements, this translates to $w = -1.03 \pm 0.16$ for the equation of state parameter of the dark energy, and $\Omega_M = 0.26 \pm 0.04$ for the matter density. Both results include also the systematic errors. This is the first direct measurement of the angular BAO signal. Our relative error determination in the angular BAO scale, including all systematics, is 9%. This is larger than the 6.5% uncertainty found by Padmanabhan et al. (2007) when comparing the scaling of the observed and fiducial power spectrum at $z = 0.5$. This difference is not totally surprising, since our method to recover the BAO position only uses the information around the BAO peak, while Padmanabhan et al. (2007) includes all scales with $k > 0.3$. The impact and analysis of systematic effects is also quite different. For example the above error

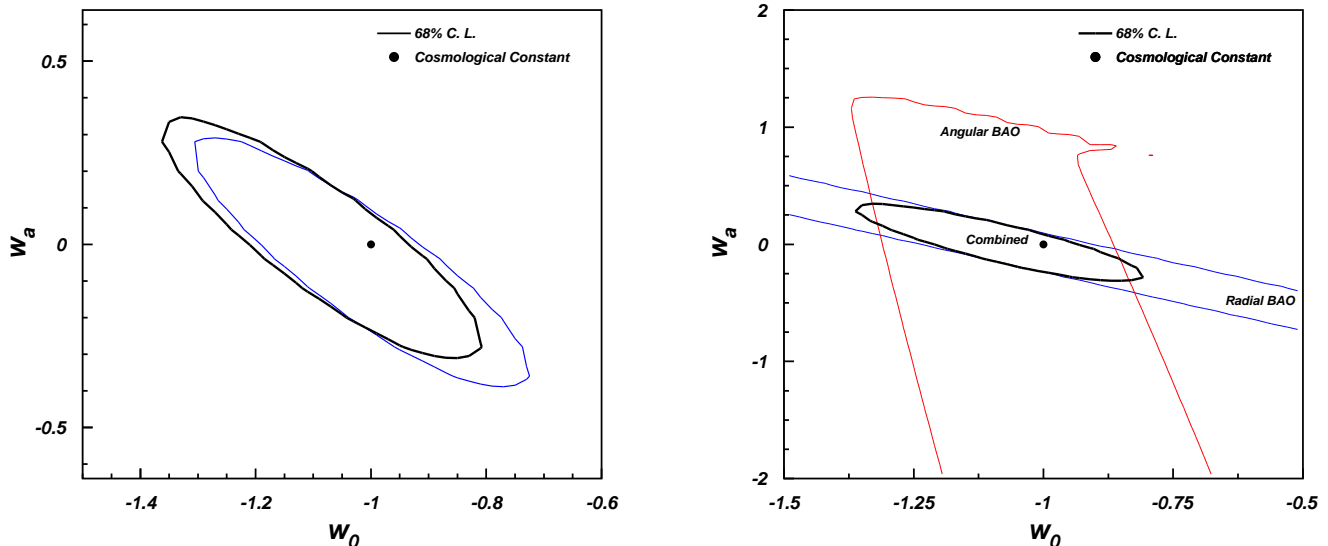


Figure 7. Left: Contribution of the new determination of the BAO scale to the cosmological constraints. The bold contour is the full combination, while the light contour is obtained when excluding the measurement at $z = 0.55$. The contribution of the new point is not negligible, and makes the constraints tighter. Right: Contribution to the cosmological constraints of the angular (light vertical contour) and radial (light diagonal contour) determinations of the BAO scale. Both determinations are complementary, and the combination (bold contour) breaks parameter degeneracies, making the constraints more precise.

in Padmanabhan does not include the photometric redshift uncertainties, while this effect dominates our systematic error (see Table 1). This measurement complements previous three-dimensional averaged and radial BAO scale determinations and makes a significant contribution to break degeneracies between cosmological parameters.

We have studied the sensitivity of the evolution of the BAO measurements performed up to date with the redshift for constraining a dark energy with equation of state variable with time, finding $\omega_a = 0.06 \pm 0.22$ when we fix all the other parameters. Therefore, data are well described by the dark energy being a cosmological constant.

This study is a confirmation of the feasibility of obtaining precise cosmological observations using photometrically determined redshifts. This allows wider and deeper galaxy samples, with the counter part of a less precise redshift. However, the smaller precision in the redshift determination is compensated with the higher statistics, allowing the obtention of precise measurements of cosmological parameters.

ACKNOWLEDGEMENTS

Funding for the SDSS and SDSS-II has been provided by the Alfred P. Sloan Foundation, the Participating Institutions, the National Science Foundation, the U.S. Department of Energy, the National Aeronautics and Space Administration, the Japanese Monbukagakusho, the Max Planck Society, and the Higher Education Funding Council for England. The SDSS Web Site is <http://www.sdss.org/>.

The SDSS is managed by the Astrophysical Research Consortium for the Participating Institutions. The Participating Institutions are the American Museum of Natural History, Astrophysical Institute Potsdam, University of

Basel, University of Cambridge, Case Western Reserve University, University of Chicago, Drexel University, Fermilab, the Institute for Advanced Study, the Japan Participation Group, Johns Hopkins University, the Joint Institute for Nuclear Astrophysics, the Kavli Institute for Particle Astrophysics and Cosmology, the Korean Scientist Group, the Chinese Academy of Sciences (LAMOST), Los Alamos National Laboratory, the Max-Planck-Institute for Astronomy (MPIA), the Max-Planck-Institute for Astrophysics (MPA), New Mexico State University, Ohio State University, University of Pittsburgh, University of Portsmouth, Princeton University, the United States Naval Observatory, and the University of Washington.

We thank the Spanish Ministry of Science and Innovation (MICINN) for funding support through grants AYA2009-13936-C06-01, AYA2009-13936-C06-03, AYA2009-13936-C06-04 and through the Consolider Ingenio-2010 program, under project CSD2007-00060.

We thank Carlos Cunha for his valuable comments about the photometric redshift.

REFERENCES

- Abazajian K. N., Adelman-McCarthy J. K., Agüeros M. A., Allam S. S., Allende Prieto C., An D., Anderson K. S. J., Anderson S. F., Annis J., Bahcall N. A., et al. 2009, *ApJS*, 182, 543
- Blake C., Collister A., Bridle S., Lahav O., 2007, *MNRAS*, 374, 1527
- Cabré A., Gaztañaga E., 2011, *MNRAS*, 412, 98
- Cabré A., Gaztañaga E., Manera M., Fosalba P., Castander F., 2006, *MNRAS*, 372, 23

- Crocce M., Cabre A., Gaztañaga E., 2010, ArXiv e-prints, 1004.4640 [astro-ph]
- Crocce M., et al., 2011, ArXiv e-prints, 1104.5236 [astro-ph]
- Cunha C. E., Lima M., Oyaizu H., Frieman J., Lin H., 2009, MNRAS, 396, 2379
- Eisenstein D. J., et al., 2001, AJ, 122, 2267
- Eisenstein D. J., et al., 2005, ApJ, 633, 560
- Gaztañaga E., A. C., Hui L., 2009, MNRAS, 399, 1663
- Gaztañaga E., Miquel R., Sánchez E., 2009, PRL, 103, 091302
- Kaiser N., Tonry J. L., Luppino G. A., 2000, PASP, 112, 768
- Kazin E. A., et al., 2010, ApJ, 710, 1444
- Komatsu E., et al., 2011, ApJS, 192, 18
- Landy S. D., Szalay A. S., 1993, ApJ, 412, 64
- Lima M., Cunha C. E., Oyaizu H., Frieman J., Lin H., Sheldon E. S., 2008, MNRAS, 390, 118
- Oyaizu H., Lima M., Cunha C. E., Lin H., Frieman J., Sheldon E. S., 2008, ApJ, 674, 768
- Padmanabhan N., et al., 2007, MNRAS, 378, 852
- Percival W. J., Cole S., Eisenstein D. J., Nichol R. C., Peacock J. A., Pope A. C., Szalay A. S., 2007, MNRAS, 381, 1053
- Percival W. J., et al., 2010, MNRAS, 401, 2148
- Reid B. A., et al., 2010, MNRAS, 404, 60
- Riess A. G., et al., 2011, ApJ, 730, 119
- Sánchez A. G., Crocce M., Cabré A., Baugh C. M., Gaztañaga E., 2009, MNRAS, 400, 1643
- Sánchez E., et al., 2011, MNRAS, 411, 277
- Schlegel D. J., et al., 2007, in American Astronomical Society Meeting Abstracts Vol. 38 of Bulletin of the American Astronomical Society, SDSS-III: The Baryon Oscillation Spectroscopic Survey (BOSS). p. 132.29
- Schlegel D. J., et al., 2009, ArXiv e-prints, 0904.0468 [astro-ph]
- The Dark Energy Survey Collaboration 2005, ArXiv e-prints, astro-ph/0510346
- Thomas S. A., Abdalla F. B., Lahav O., 2011, MNRAS, 412, 1669
- Tyson J. A., Wittman D. M., Hennawi J. F., Spergel D. N., 2003, Nuclear Physics B Proceedings Supplements, 124, 21
- York D. G., et al., 2000, AJ, 120, 1579